

## Simulation study of magnetorheological testing cell design by incorporating all basic operating modes

Mohd J. Mughni<sup>1a</sup>, Saiful A. Mazlan<sup>\*1</sup>, Hairi Zamzuri<sup>2b</sup>, Izyan I.M. Yazid<sup>1c</sup>  
and Mohd A.A. Rahman<sup>1d</sup>

<sup>1</sup>Malaysia-Japan International Institute of Technology, Universiti Teknologi Malaysia,  
Jalan Semarak, 54100 Kuala Lumpur, Malaysia

<sup>2</sup>Vehicle System Engineering Research Laboratory, Universiti Teknologi Malaysia,  
Jalan Semarak, 54100 Kuala Lumpur, Malaysia

(Received May 28, 2013, Revised January 9, 2014, Accepted January 12, 2014)

**Abstract.** Magnetorheological (MR) fluid is one of the field-responsive fluids that is of interest to many researchers due to its high yield stress value, which depends on the magnetic field strength. Similar to electrorheological (ER) fluid, the combination of working modes is one of the techniques to increase the performance of the fluids with limited focus on MR fluids. In this paper, a novel MR testing cell incorporated with valve, shear and squeeze operational modes is designed and constructed in order to investigate the behaviour of MR fluid in combined mode. The magnetic field distribution in the design concept was analyzed using finite element method in order to verify the effective areas of each mode have the acceptable range of flux density. The annular gap of valve and shear were fixed at 1 mm, while the squeeze gap between the parallel circular surfaces was varied up to 20 mm. Three different coil configurations, which were made up from 23 SWG copper wires were set up in the MR cell. The simulation results indicated that the magnetic field distributed in the squeeze gap was the highest among the other gaps with all coils were subjected to a constant applied current of 1 A. Moreover, the magnetic flux densities in all gaps were in a good range of magnitude based on the simulations that validated the proposed design concept. Hence, the 3D model of the MR testing cell was designed using Solidworks for manufacturing processes.

**Keywords:** magnetorheological fluid; combination mode; finite element method; design; testing cell; simulation

### 1. Introduction

Magnetorheological (MR) fluid is a suspension of magnetisable micron-sized particles in a carrier liquid such as hydrocarbon oil and silicone oil (Jolly *et al.* 1999). Under the absence of magnetic field, the solid particles are randomly dispersed in the carrier medium. In this original

---

\*Corresponding author, Ph.D., E-mail: [amri.kl@utm.my](mailto:amri.kl@utm.my)

<sup>a</sup> Ph.D. Student, E-mail: [mjamalullail2@live.utm.my](mailto:mjamalullail2@live.utm.my)

<sup>b</sup> Ph.D., E-mail: [hairi.kl@utm.my](mailto:hairi.kl@utm.my)

<sup>c</sup> Ph.D. Student, E-mail: [iiryani3@live.utm.my](mailto:iiryani3@live.utm.my)

<sup>d</sup> Ph.D., E-mail: [azizi.kl@utm.my](mailto:azizi.kl@utm.my)

state of MR fluid, the viscosity remains unchanged and the fluid is free to flow. The remarkable change to a semi-solid state is occurred when the fluid is energized with a certain magnitude of applied magnetic field. The rheological change is reversible and can be controlled by using electromagnetic coil as a magnetic field generator. Unlike permanent magnet, the strength of the generated magnetic field can easily be controlled depending on the supplied current. However, Bose and Ehrlich (2012) recently have combined the electromagnet and permanent magnet where the latter serve as a fail-safe functioning part.

Inter-particles studies previously done by numerous researchers in the field (Hagenbuchle and Liu 1997, Tang *et al.* 2000, Carletto and Bossis 2003, Ismail *et al.* 2012) showed that under the influence of magnetic field, each iron particle will create a magnetic dipole resulting the attraction of particles with the different poles and repulsion with the same charge poles. The process leads to a formation of chains of particles and became thick columns of chains. These chains were crossing the gap between the two walls of magnetic materials. The resistance created from the columns of chains prevented the fluid from flowing hence the determination of the yield stress. Genc and Phule (2002) showed that the stresses produced by MR fluid with larger size of particles and higher volume fraction were stronger than the sample with smaller particles and lower volume fraction respectively. Moreover, the viscosity of the fluid increased proportionally with the magnetic field.

The operational modes of MR fluid were familiarly recognized as flow or valve mode, shear mode and squeeze mode (Wang and Meng 2001) where the stress produced by each mode was having different values. The working principle of each operational mode is illustrated in Fig. 1. In valve mode (see Fig. 1(a)), the gap, which can be represented by either annular or radial flow paths were made up from two fixed parallel wall-plates and the MR fluid was flowing through the walls by gradient of pressure. The shear mode takes place if one of the walls is moved relatively with the other wall which is fixed, as shown in Fig 1(b). The squeeze mode is occurred when the fluid is being compressed or decompressed by the two wall-plates (see Fig. 1(c)). Besides of these three basic operating modes, a new mode called the gradient-pinch mode (see Fig. 1(d)) was discovered recently by Goncalves and Carlson (2009), where similar to valve mode, the fluid flows by a gradient of pressure but the channel effective gap is reduced upon the increased of applied current. Hence, the gradient of pressure increase as the flow gap decreases. In all modes excluding the gradient-pinch mode, the direction of magnetic flux is always perpendicular to the plates. The three basic working modes formerly stated are also existed in electrorheological (ER) fluids which use electric field as an external stimulus instead of magnetic field. Among these modes, the stress produced by squeeze mode in ER fluid was found to be higher than the other modes (Tian *et al.* 2002, Mazlan *et al.* 2009). The result was similar to MR fluids, where the squeeze mode considerably enhanced the operation performance in terms of yield stress value. Wang *et al.* (2011) found that the tensile yield stress in squeeze mode was about four times higher than the yield stress produced by shear mode. In another study of squeeze mode under nonuniform magnetic field, Guo *et al.* (2013) affirmed that the normal stress during compression was found to be larger than in shear or valve mode while considering the existence of sealing and strengthening effect.

The improvement of stress magnitude has been continuously studied particularly in combination of working modes technique. Gavin (1998) has developed non-dimensional model of polynomial equations to predict the behaviour of ER fluids under combination of valve and shear modes. Similar combination of these two modes was done for MR fluids by Wereley and Pang (1998), where non-dimensional analysis has been made to characterize the damping performance and prove the design concept at model-scale. The analysis has been experimentally validated in a

later study by Hong *et al.* (2008). He concluded that the non-dimensional parameters studied can be applied for both ER and MR fluids by using correct consideration of the active length parameter. The combination of shear and squeeze modes was done recently by El Wahed and McEwan (2011) who studied the performance of MR fluids in under oscillatory loading with mechanical frequency in the range 2-25 Hz. The same combination of operational modes was also reported by Yazid *et al.* (2014) but under quasi-static loading with a constant speed of 50 mm/min. They proved that the damping force achieved by using a mixed mode damper was higher than that of a single mode damper. Brigley *et al.* (2007) proposed an MR isolator with combination of valve, shear and squeeze modes but they only used one single coil to create the magnetic field which is not strong enough and the effective areas were too small. In another recent study, Imaduddin *et al.* (2013) has proposed a combination of multiple valve modes (annular and radial gaps) by using a meandering pattern in the flow channel of the MR fluid. They found that the pressure drop can be achieved higher than 2.5 MPa with only 50 mm of outer diameter of a compact MR valve.

In this paper, the combination of modes is emphasized by clearly design the valve, shear and squeeze mode in a single cell. Consequently, the effective areas were clear effect of pressure-driven mode, direct-shear mode and pure squeeze mode. Furthermore, instead of using a single winding coil (Brigley *et al.* 2007), three induction coils are used in this study to increase the magnetically active zone in the MR cell. The design concept was analysed with various parameters input to increase the efficacy of MR testing cell in terms of magnetic flux and manufacturing process.

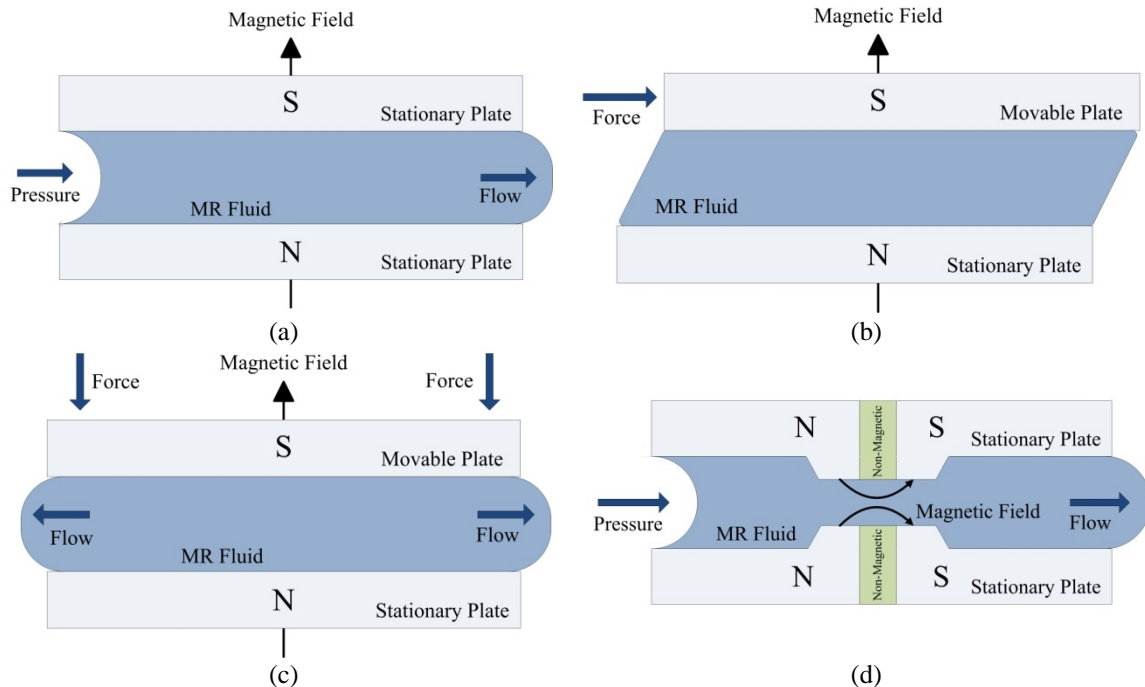


Fig. 1 Three basic operational modes of MR fluids include (a) valve mode, (b) shear mode and (c) squeeze mode, and the recently discovered (d) gradient pinch mode

## 2. Structure and working principle of MR testing cell

### 2.1 MR fluid

Three different densities of commercial MR fluid were used in this study. All hydrocarbon-based of MR fluids were produced by Lord Corporation under the code name of MRF-122EG, MRF-132DG and MRF-140CG with weight fraction of solids content were 0.72, 0.81 and 0.85 respectively. The size of the iron particles in the fluids was in the range of 1-20  $\mu\text{m}$ . Based on the data provided by Lord, the MR fluids have a response time less than 5 ms. Nevertheless, it may be varied depending on the design of the device. For example, a short and a long stroke dampers produced by the same manufacturer has a response time less than 15 ms and recently, the behaviour of both devices have been successfully predicted through mathematical modelling by Zeinali *et al.* (2013). The typical properties of both MR fluids are summarized in Table 1. Some variants of commercial MR fluids were existed in the market and were used by researchers in their studies (Jolly *et al.* 1999, Mazlan *et al.* 2011, Wang *et al.* 2011) while some researchers preferred to utilize a home-made MR fluids (Genc and Phule 2002, El Wahed and McEwan 2011).

### 2.2 The structure of MR cell

The MR testing cell was intentionally designed to be able to operate under three different operational modes simultaneously which include valve, shear and squeeze modes. Similar self-constructed systems have been done by Mazlan *et al.* (2009) and El Wahed and McEwan (2011) to study the behaviour of MR fluids. However, Mazlan and co-workers were concentrated on squeeze mode alone where the MR fluid was sandwiched between circular disk areas of two separated cylinder of carbon steels arranged vertically in a monotonic unidirectional compression (see Fig. 2(a)). The effective area of MR fluids was defined between these two parallel surfaces where the magnetic flux lines generated by the electromagnet coil of lower cylinder were guided to cross over the fluids to the upper cylinder. Moreover, the MR fluid was compressed from 2 to 0.4 mm of squeeze gap height.

Table 1 Physical properties of commercial MR fluids

Code name	MRF-122EG	MRF-132DG	MRF-140CG
Solids content by weight	72%	80.98%	85.44%
Base fluids	Hydrocarbon	Hydrocarbon	Hydrocarbon
Colour	Dark gray	Dark gray	Dark gray
Viscosity @ 40° with slope 800-1200 $\text{sec}^{-1}$	0.061 Pa.s	0.112 Pa.s	0.28 Pa.s
Density range	2.28-2.48 $\text{g/cm}^3$	2.95-3.15 $\text{g/cm}^3$	3.54-3.74 $\text{g/cm}^3$
Max. yield stress	35 kPa	50 kPa	60 kPa
Response time	< 5 ms	< 5 ms	< 5 ms
Operating temperature	-40 to +130 °C	-40 to +130 °C	-40 to +130 °C
Flash point	> 150 °C	> 150 °C	> 150 °C

In a later study, El Wahed and co-worker combined the squeeze and shear modes in a single MR cell (see Fig. 2(b)). Instead of having one effective area in the form of disk shape, the shear area which is in a cylindrical hollow shape was added in the experiment. The design of lower cylinder was a cuplike shape to sink the upper cylinder in MR fluids. The purpose of the immersion was to formulate the shearing deformation of the activated MR fluids between the inner wall of the cuplike cylinder and the wall of upper cylinder. The magnetic circuit was arranged with two electromagnetic coils wound around the lower cylinder and the other one around the upper cylinder. These coils were separately controllable in order to activate the MR fluids either in single or mixed mode. Furthermore, the MR cell was continuously in cyclic motion with the range frequency of 2-25 Hz. The range of the compression gap was 0.1 to 2 mm for squeeze and 2 mm fixed gap of shear.

In this study, the previous concept of mixed mode is maintained while another operational mode is added. An annular flow channel is designed by integrating a ring-shaped carbon steel with 1 mm of non-magnetic spacers on the upper cylinder, which is called piston rod, allowing the activation of valve mode. Fig. 3(a) depicts the schematic diagram of the new MR testing cell with triple working modes and three induction coils that can be controlled independently. Another ring without spacers which attached completely to the piston rod was also prepared for the test of only shear and squeeze mode enabled (see Fig. 3(b)). Two of the coils were placed on the piston rod to increase the efficacy of shear mode and also to control separately the effective areas desired. The piston rod was submerged in the reservoir of MR fluids made up from a steel sleeve cylinder connected to the lower bobbin of MR cell. The reservoir of the fluid was moved by the controlled rig machine while the piston was left stationary. The annular gap between the piston rod and the reservoir cup was maintained to 1 mm to ensure the optimized effect of shearing deformation.

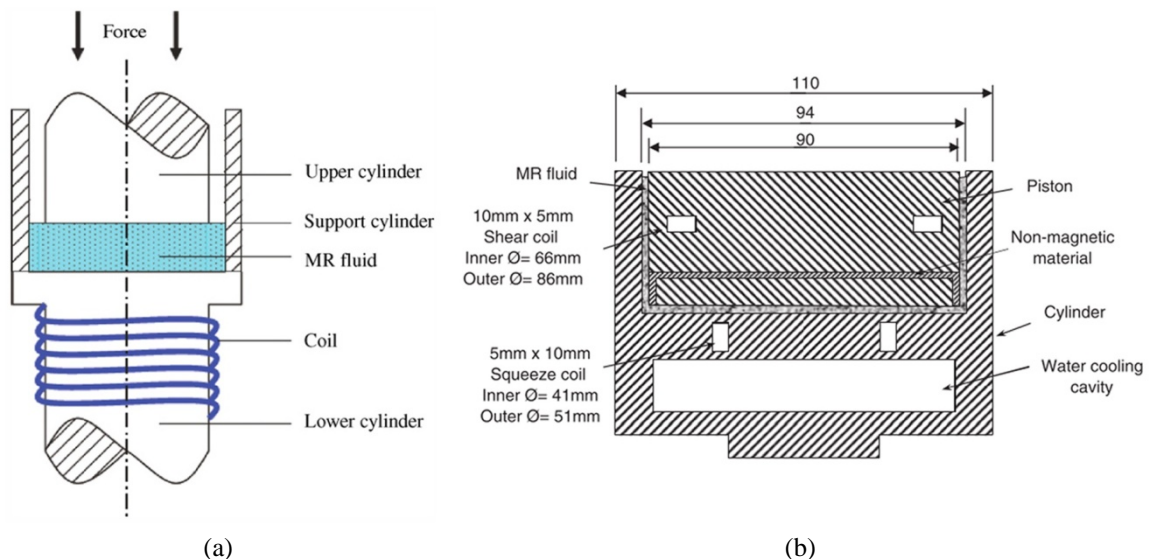


Fig. 2 MR testing cell previously done by (a) Mazlan *et al.* (2009) with squeeze mode and (b) El Wahed and McEwan (2011) with combination of shear and squeeze modes

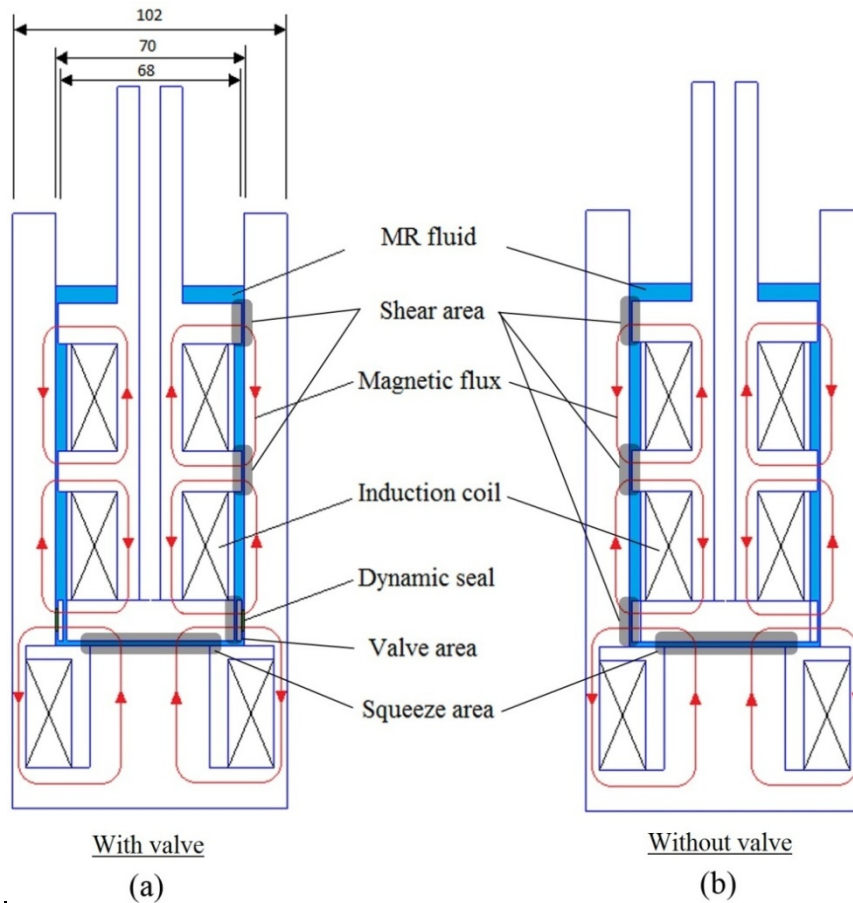


Fig. 3 The schematic diagrams of MR testing cell (a) with three working modes; valve, shear and squeeze modes and (b) with two working modes; shear and squeeze modes (without valve mode)

### 2.3 Magnetic flux path

The design concept of the novel MR testing cell capable to operate with three working modes was verified with Finite Element Method Magnetics (FEMM). The design had previously undergone several modifications and were all simulated in the FEMM software package in searching of the optimize magnetic field distribution in each effective area. Finite element analysis was widely used by other researchers in the field of MR fluids (Goncalves and Carlson 2009, Mazlan *et al.* 2009, El Wahed and McEwan 2011, Wang *et al.* 2011) to study the magnetic field behaviour in the MR devices.

The positions of non-magnetic and magnetic materials play an important role in guiding the magnetic flux path into the effective areas. For that purpose, the existence of stainless steel (non-magnetic material) in the lower part of MR testing cell was considered in order to guide the path of magnetic flux from the bobbin across the MR fluid to the piston rod and looped to the sleeve cylinder and to the core of the bobbin. As shown in Fig. 4, three different loops were clearly prevailed in the simulation and efficiently guided to the effective areas. To ensure a maximum MR

effect with the formation of chains of particles, the direction of the magnetic flux lines must be perpendicular to the surfaces of the effective areas (Tang *et al.* 2000, Carletto and Bossis 2003).

Moreover, with multiple induction coils in a single MR cell, the determination of polarity for each coil was given careful consideration during the design simulation phase. All possibilities of polarization have been simulated in the FEMM to select the best configuration where the magnetic flux densities concentrated on the effective areas. Fig. 3 showed the chosen polarization for different induction coil of MR testing cell represented by the magnetic flux loops.

### 3. Results and discussion

The experiment was intended to both monotonic and cyclic compression studies with small initial circular surfaces gaps in the range 2-20 mm. In this study, monotonic compression was emphasized with the initial squeeze gap was set to 2 mm and the current supplies to generate the magnetic field to the induction coils were in the range 0-1 A. The maximum values of current were based on the diameter of the copper wire wound around the MR cell as different size of copper wire gave different maximum current permitted. Thus, 23 SWG of insulated copper wire which has the diameter of 0.67 mm was selected for the study.

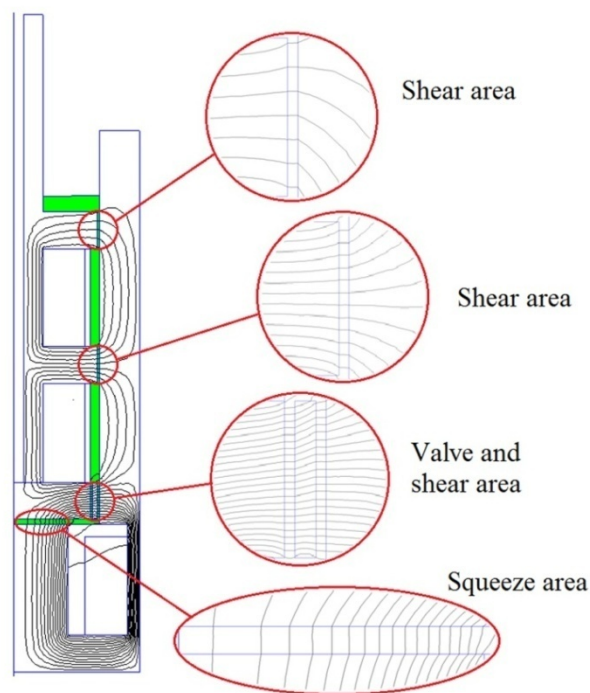


Fig. 4 Middle half of the MR testing cell showing the simulated magnetic flux path with three different loops and the effective areas of MR fluid

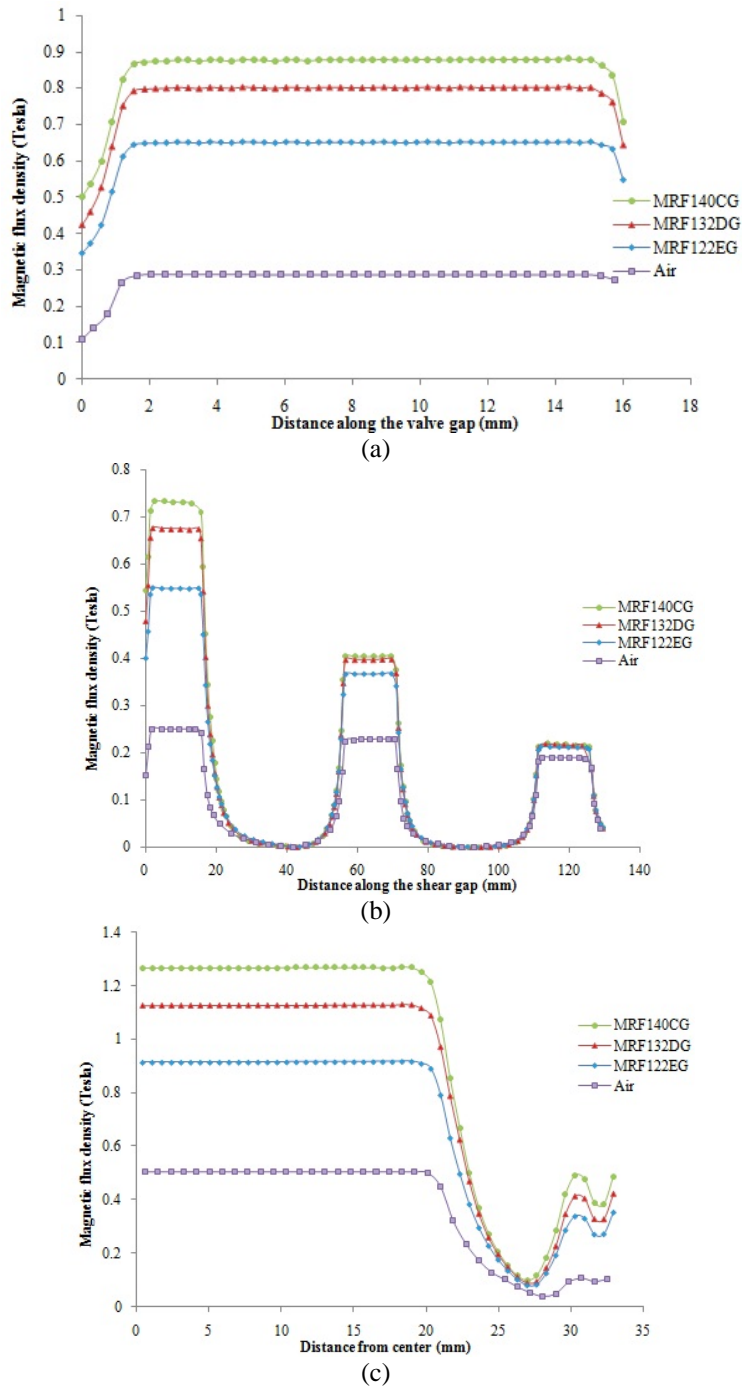


Fig. 5 Magnetic flux density versus distance along the surfaces of effective areas for (a) valve, (b) shear and (c) squeeze gaps for different MR fluids compared to the air

Fig. 5 represents the simulated magnetic flux density along the surfaces of effective areas for different commercial MR fluids. The applied current was kept constant at 1 A for each coil configuration. The results have shown the optimized values of magnetic flux density. The distance of the effective area of valve, shear and squeeze were 15, 15 each with a total of 45 and 44 mm, respectively. Each curve was plotted with 100 points in the simulation to achieve a nearly uniform distribution of magnetic field and the mean value of magnetic flux density along the effective gap was calculated.

For every effective area, the use of MRF-140CG always attained the highest value of magnetic flux density. For example in the valve gap, the average values of magnetic flux density for MRF-122EG, MRF-132DG and MRF-140CG were 0.65, 0.80 and 0.87 Tesla, respectively. This is due to the fact that, the MRF-140CG has about 85% of iron solid particles content by weight whereas the MRF-122EG and MRF-132DG have 72 and 81%, respectively, leading to different values of magnetic permeability ( $\mu$ ) and saturation magnetization ( $\mu_0 M_s$ ). Genc and Phule (2002) have demonstrated that the higher volume fraction of particles, the higher value of saturation magnetization that would increase the yield stress value of the MR fluids. Among all MR fluids properties (see Table 1), MRF-140CG has about 60kPa of yield stress value, higher than the other fluids. Furthermore, the magnetic field strength ( $H$ ) of each MR fluids would also be different relatively to the magnetic flux density value.

For the rest of the results, MRF-132DG has been selected to be used for the introductory experiment as the result consistencies produced by this type of fluid has been proven by other researchers (Ismail *et al.* 2012, Mazlan *et al.* 2009, 2011, Nguyen *et al.* 2008). Fig. 6 shows the variation of current supplied to all coils of MR testing cell with initial squeeze gap at 2 mm. The result of the simulation showed that the magnitude of flux density increased as the current applied to an individual coil increased at all effective areas. Even though each coil was given the same current input, for example 1 A, the average value of magnetic flux density for each effective area was not the same i.e., 0.85 Tesla for valve gap, 0.72, 0.42 and 0.22 Tesla in the shear gap and 1.21 Tesla in the squeeze gap. Indeed, the structure design of MR testing cell indicated that the piston rod and the lower bobbin were different in core diameter. If the top coil has the same number of turns as the coil at the lower bobbin, the core with larger diameter would take much longer wire to wind up thus more resistance and more voltage needed to be supplied. The higher voltage would proportionally increase the value of magnetic flux density. The dependence of the MR fluid behaviour with applied current was in good agreement with other researchers (Mazlan *et al.* 2009, El Wahed and McEwan 2011, Bose and Ehrlich 2012). There were also numerous prediction methods already suggested by some researchers through mathematical modelling which correlate the applied current and force response either in linear (Zeinali *et al.* 2013) or rotary dampers (Bhowmik *et al.* 2013).

Fig. 7 represents the variation of initial compression gap from 2.5 to 0.5 mm with the effect on the simulated values of the average magnetic flux density in each effective area. All coils were given the same value of applied current. The simulation tests were repeated for different values of current supplied by using the same type of MR fluid. The results show that the decreasing distance of initial squeeze gap will increase the magnetic flux density values in all effective areas of valve (see Fig. 7(a)), shear (see Fig. 7(b)) and squeeze (see Fig. 7(c)). However, the values of magnetic flux density in shear area (see Fig. 7(b)) were obtained by the summation of the average of magnetic flux density value at the top, middle and bottom of shear effective areas. In contrast to what one would expect intuitively, the addition of three effective areas resulted to plateau curves rather than steep slopes as in the result of valve area Fig. 7(a) and squeeze area in Fig. 7(c). The

contribution of magnetic flux density in shear area for different initial squeeze gaps is represented in Fig. 8.

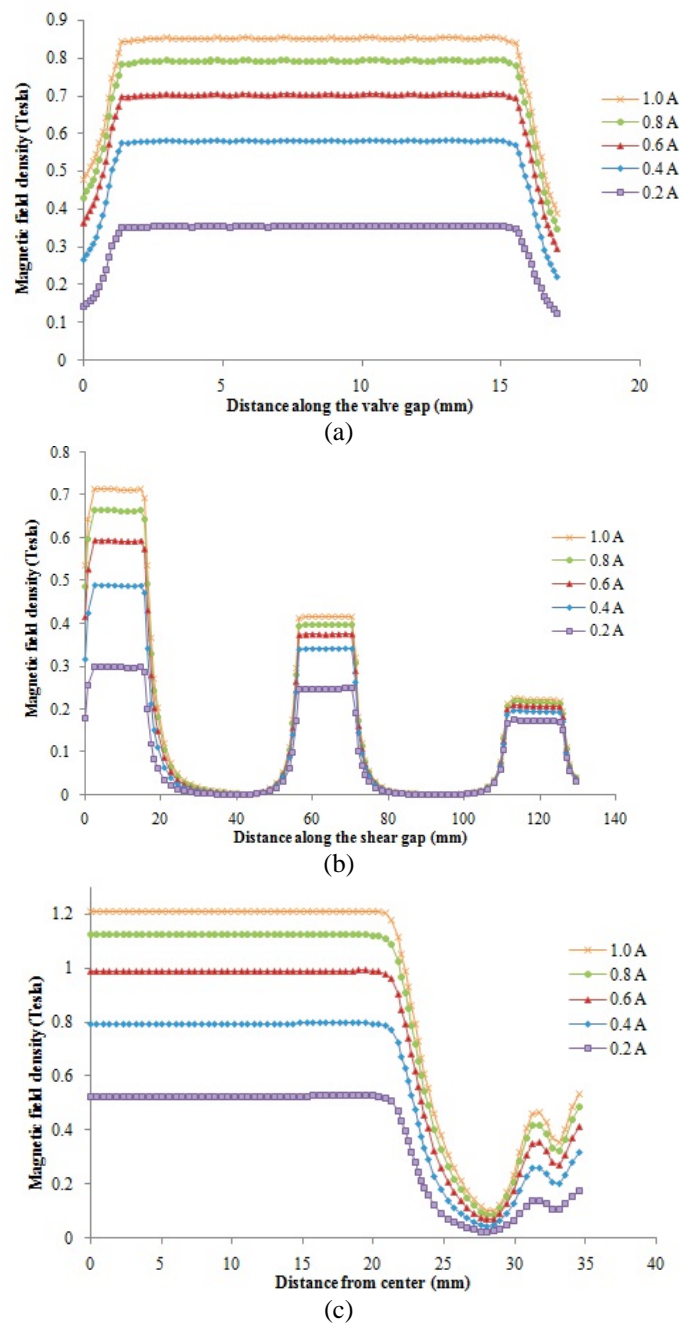


Fig. 6 Magnetic flux density versus distance along the surfaces of effective areas for (a) valve, (b) shear and (c) squeeze gaps for different applied currents

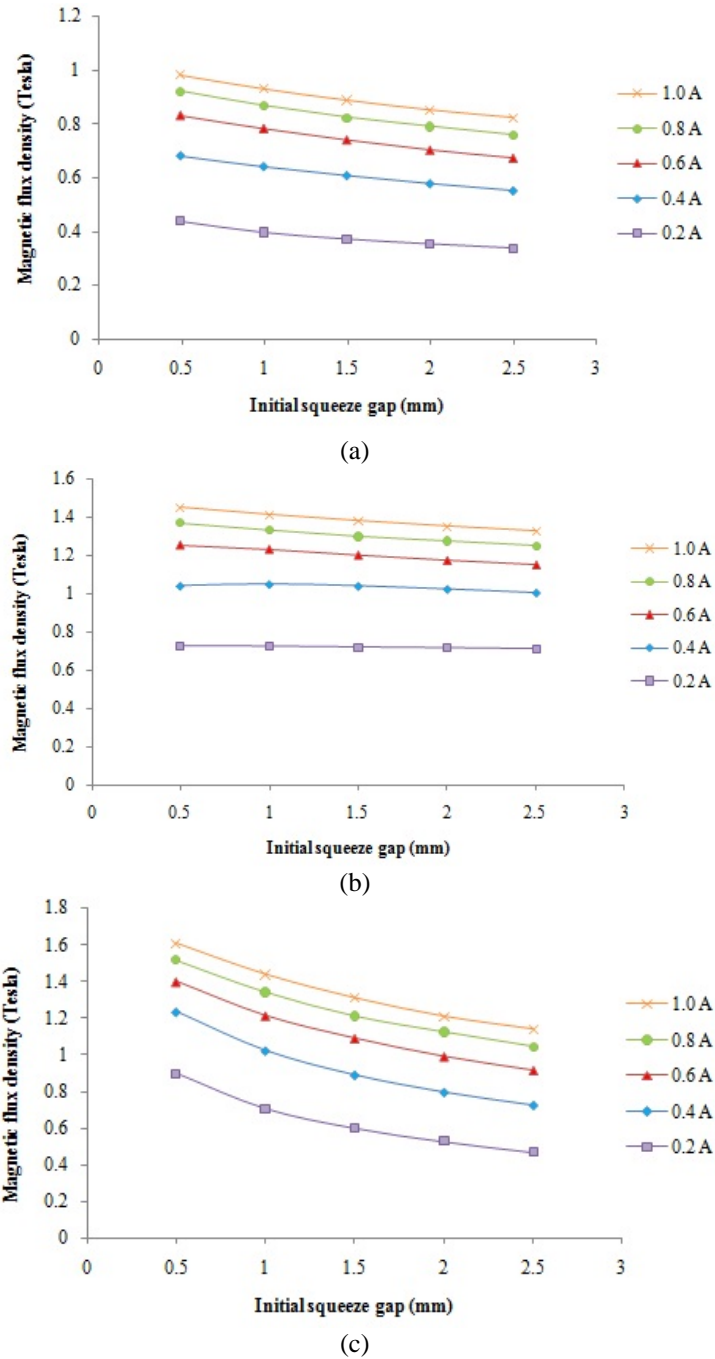


Fig. 7 Magnetic flux density at the effective area of (a) valve, (b) shear and (c) squeeze for different initial squeeze gaps for different applied currents

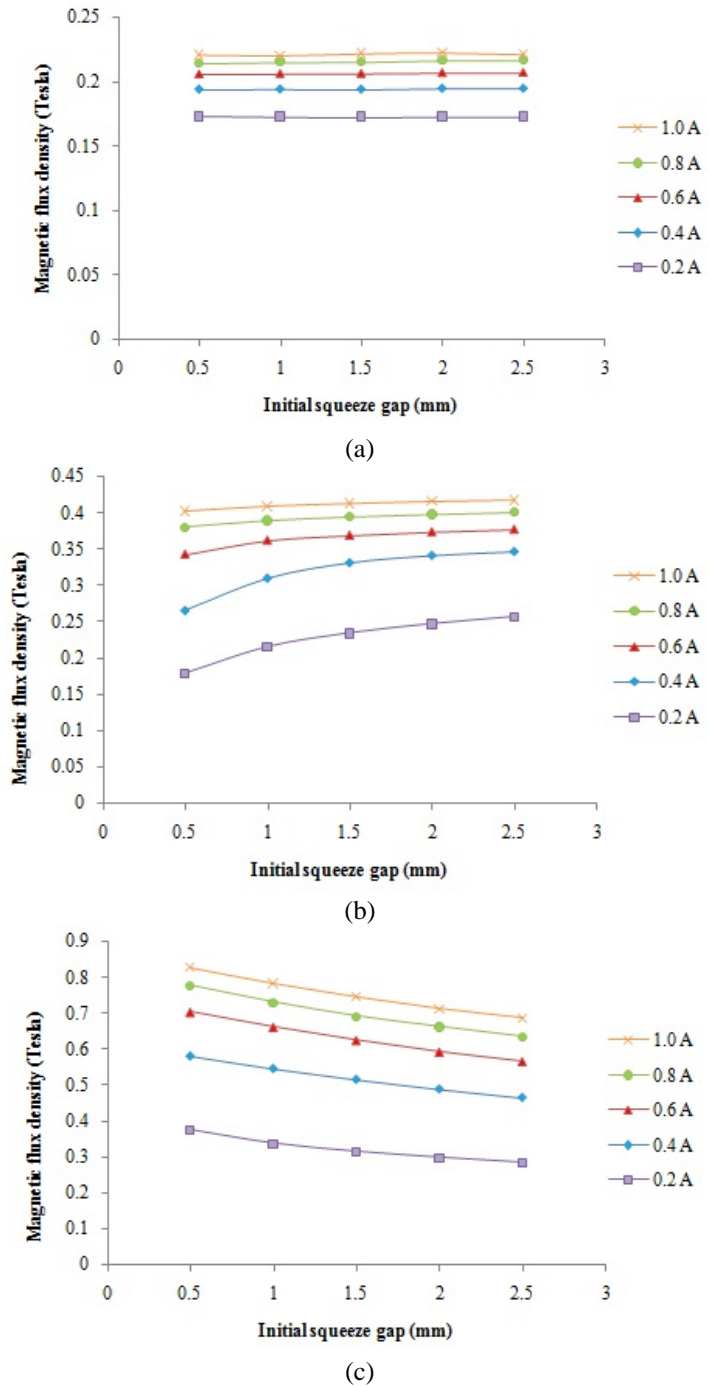


Fig. 8 Magnetic flux density at the (a) top, (b) middle and (c) bottom of shear effective areas for different initial squeeze gaps for different applied currents

The average value of flux density at the top of shear area indicated insignificant variation upon the different initial squeeze gaps applied (see Fig. 8(a)). However, at the middle of shear area, the result shows contrary effect where the magnetic flux density decreased upon the decreasing of initial squeeze gap (see Fig. 8(b)). Indeed, the highest contribution of magnetic flux density in shear area was at the bottom, similarly represented in Fig. 6(b), and significant increased of magnetic flux density was shown in the result after decreasing the initial gap values (see Fig. 8(c)). Despite of the fact the length of each shear effective area were the same, the three coils which provide the magnetic flux density, have distinct configurations. Moreover, the magnitude of flux density in these simulation results were in a good range based on the available data supplied by Lord Corporation and other researchers (Mazlan *et al.* 2009, El Wahed and McEwan 2011, Mazlan *et al.* 2011, Wang *et al.* 2011).

From the values of average magnetic flux density obtained, the values of yield stress can be estimated by applying the approximate polynomial equation for MRF-132DG constructed by Nguyen *et al.* (2008)

$$\tau_Y(B) = 52.962B^4 - 176.51B^3 + 158.79B^2 + 13.708B + 0.1442 \quad (1)$$

where  $\tau_Y$  is the yield stress in kPa and  $B$  is the magnetic flux density in Tesla. Table 2 is the example of summarized average values of  $B$  in different effective areas when all coils are subjected to 1 A of DC current and the values of  $\tau_Y$  calculated using Eq. (1). Fig. 9 shows the relationship between the accumulated yield stress value for all effective areas and the initial squeeze gap for different applied current. The novel MR testing cell with three working modes is estimated to provide a yield stress value up to 5000 kPa with 1 A of current supplied to all coils.

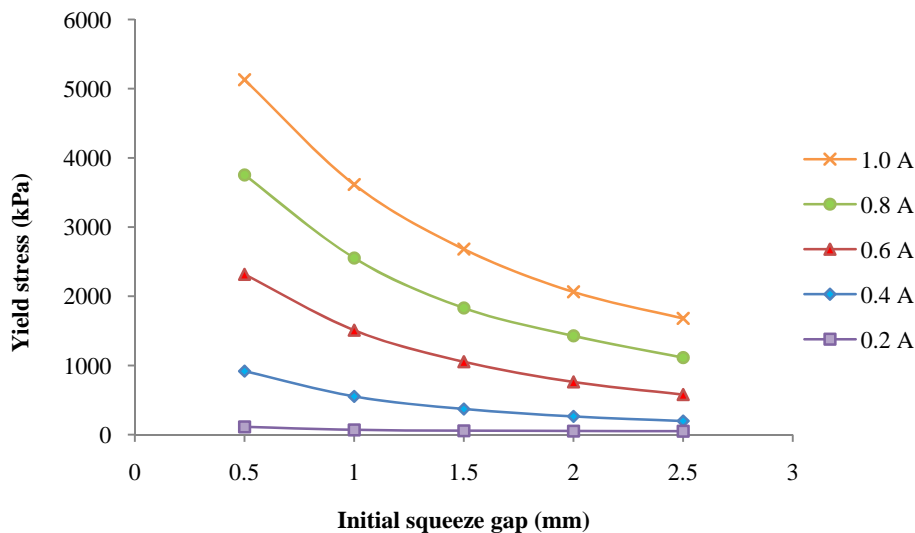


Fig. 9 Estimated yield stress value versus initial squeeze gap for different applied currents

Table 2 Summarized values of magnetic flux density  $B$  when all coils are supplied with DC current of 1 A

Initial squeeze gap (mm)	Magnetic flux density $B$ (Tesla) in the effective area of					Accumulated magnetic flux density $B$ (Tesla)	Yield stress $\tau_y$ (kPa)
	valve	shear - top	shear - middle	shear - bottom	squeeze		
0.5	0.9806	0.2211	0.4028	0.8287	1.6088	4.0420	5130.34
1.0	0.9297	0.2206	0.4095	0.7847	1.4385	3.7830	3615.41
1.5	0.8875	0.2221	0.4135	0.7470	1.3093	3.5794	2682.67
2.0	0.8510	0.2227	0.4163	0.7147	1.2081	3.4128	2064.87
2.5	0.8223	0.2214	0.4182	0.6888	1.1385	3.2892	1681.05

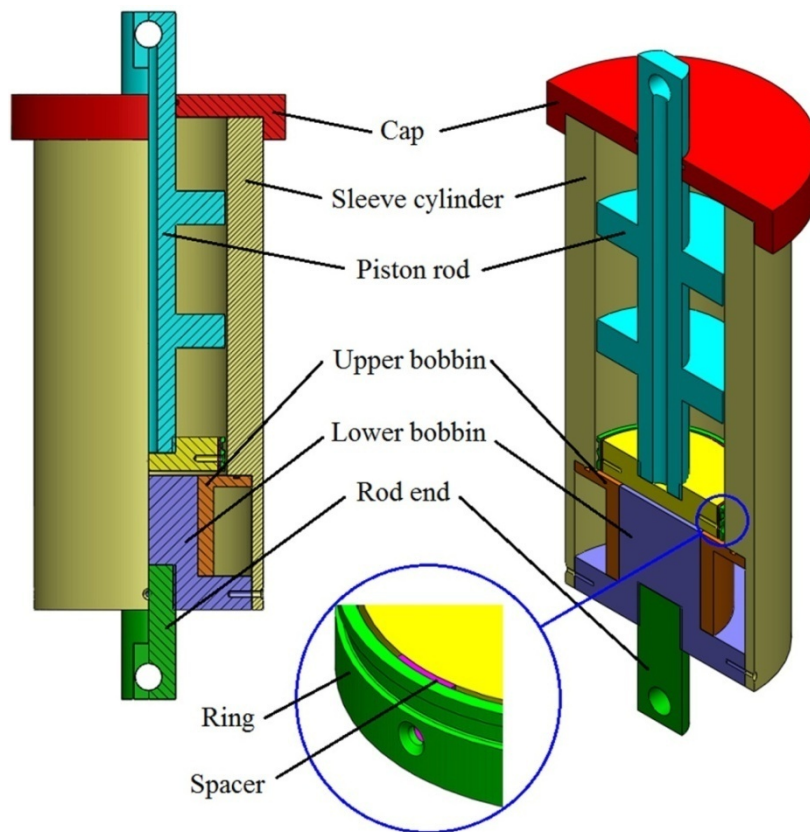


Fig. 10 3D design of the novel MR testing cell

In conjunction with the optimum flux density obtained for each effective area after several design modifications, the actual design in 3D was followed by using Solidworks software illustrated in Fig. 10.

#### 4. Conclusions

In this paper, an MR testing cell with combination of valve, shear and squeeze mode was carefully designed in parallel with the simulation phase. Three different MR fluids commercially available and different coil configurations such as the selection of wire diameter and the number of turns were simulated in order to obtain the best range of magnetic flux density along the effective areas. The simulation results showed that the obtained value of magnetic flux densities in valve, shear and squeeze gaps were comparable to other researchers as well as its dependence with the applied currents. Moreover, the decreasing of initial squeeze gap showed an increase in the average value of magnetic flux density in all effective areas except at the top and the middle of shear area. The estimated value of total yield stress in all effective areas upon the decreasing value of initial squeeze gap was also presented. The proposed magnetic circuit design is presently validated and the 3D model is designed for fabrication.

#### Acknowledgments

The research work in this paper was financially supported by Ministry of Education Malaysia under the Fundamental Research Grant Scheme (FRGS) with vote no. 4L094.

#### References

- Bhowmik, S., Weber, F. and Hogsberg, J. (2013), "Experimental calibration of forward and inverse neural networks for rotary type magnetorheological damper", *Struct. Eng. Mech.*, **46**(5), 673-693.
- Bose, H. and Ehrlich, J. (2012), "Magnetorheological dampers with various designs of hybrid magnetic circuits", *J. Intel. Mat. Syst. Str.*, **23**(9), 979-987.
- Brigley, M., Choi, Y.T., Wereley, N.M. and Choi, S.B. (2007), "Magnetorheological isolators using multiple fluid modes", *J. Intel. Mat. Syst. Str.*, **18**(12), 1143-1148.
- Carletto, P. and Bossis, G. (2003), "Field-induced structures and rheology of a magnetorheological suspension confined between two walls", *J. Phys. - Condens. Mat.*, **15**(15), S1437-S1449.
- El Wahed, A.K. and McEwan, C.A. (2011), "Design and performance evaluation of magnetorheological fluids under single and mixed modes", *J. Intel. Mat. Syst. Str.*, **22**(7), 631-643.
- Gavin, H.P. (1998), "Design method for high-force electrorheological dampers", *Smart Mater. Struct.*, **7**(5), 664-673.
- Genc, S. and Phule, P.P. (2002), "Rheological properties of magnetorheological fluids", *Smart Mater. Struct.*, **11**(1), 140-146.
- Goncalves, F.D. and Carlson, J.D. (2009), "An alternate operation mode for MR fluids-magnetic gradient pinch", *J. Phys.: Conf. Ser.*, **149**(1), 012050.
- Guo, C., Gong, X., Xuan, S., Qin, L. and Yan, Q. (2013), "Compression behaviors of magnetorheological fluids under nonuniform magnetic field", *Rheol. Acta*, **52**(2), 165-176.
- Hagenbuchle, M. and Liu, J. (1997), "Chain formation and chain dynamics in a dilute magnetorheological fluid", *Appl. Optics*, **36**(30), 7664-7671.
- Hong, S.R., Wereley, N.M., Choi, Y.T. and Choi, S.B. (2008), "Analytical and experimental validation of a nondimensional Bingham model for mixed-mode magnetorheological dampers", *J. Sound Vib.*, **312**(3), 399-417.
- Imaduddin, F., Mazlan, S.A., Zamzuri, H. and Yazid, I.I.M. (2013), "Design and performance analysis of a compact magnetorheological valve with multiple annular and radial gaps", *J. Intel. Mat. Syst. Str.*, DOI:

10.1177/1045389X13508332.

- Ismail, I., Mazlan, S.A., Zamzuri, H. and Olabi, A.G. (2012), "Fluid-particle separation of magnetorheological fluid in squeeze mode", *Jpn. J. Appl. Phys.*, **51**(6), 067301.
- Jolly, M.R., Bender, J.W. and Carlson, J.D. (1999), "Properties and applications of commercial magnetorheological fluids", *J. Intel. Mat. Syst. Str.*, **10**(1), 5-13.
- Mazlan, S.A., Ismail, I., Zamzuri, H. and Abd Fatah, A.Y. (2011), "Compressive and tensile stresses of magnetorheological fluids in squeeze mode", *Int. J. Appl. Electrom.*, **36**(4), 327-337.
- Mazlan, S.A., Issa, A., Chowdhury, H.A. and Olabi, A.G. (2009), "Magnetic circuit design for the squeeze mode experiments on magnetorheological fluids", *Mater. Design*, **30**(6), 1985-1993.
- Nguyen, Q.H., Choi, S.B. and Wereley, N.M. (2008), "Optimal design of magnetorheological valves via a finite element method considering control energy and a time constant", *Smart Mater. Struct.*, **17**(2), 025024.
- Tang, X., Zhang, X., Tao, R. and Rong, Y.M. (2000), "Structure-enhanced yield stress of magnetorheological fluids", *J. Appl. Phys.*, **87**(5), 2634-2638.
- Tian, Y., Meng, Y., Mao, H. and Wen, S. (2002), "Electrorheological fluid under elongation, compression and shearing", *Phys. Rev. E.*, **65**(3), 031507.
- Wang, H., Bi, C., Kan, J., Gao, C. and Xiao, W. (2011), "The mechanical property of magnetorheological fluid under compression, elongation and shearing", *J. Intel. Mat. Syst. Str.*, **22**(8), 811-816.
- Wang, J. and Meng, G. (2001), "Magnetorheological fluid devices: principles, characteristics and applications in mechanical engineering", *P. I. Mech. Eng. L-J. Mat.*, **215**(3), 165-174.
- Wereley, N.M. and Pang, L. (1998), "Nondimensional analysis of semi-active electrorheological and magnetorheological dampers using approximate parallel plate models", *Smart Mater. Struct.*, **7**(5), 732-743.
- Yazid, I.I.M., Mazlan, S.A., Kikuchi, T., Zamzuri, H. and Imaduddin, F. (2014), "Design of magnetorheological damper with a combination of shear and squeeze modes", *Mater. Design*, **54**, 87-95.
- Zeinali, M., Mazlan, S.A., Abd Fatah, A.Y. and Zamzuri, H. (2013), "A phenomenological dynamic model of a magnetorheological damper using a neuro-fuzzy system", *Smart Mater. Struct.*, **22**(12), 125013.